Hindawi
Mathematical Problems in Engineering
Volume 2022, Article ID 1143374, 14 pages
https://doi.org/10.1155/2022/1143374

Research Article

The Research of the Overlapping Decentralized Guaranteed Cost Hybrid Control Method for Adjacent Buildings with Uncertain Parameters

Qinghu Xu,[1,2,3] Xuezhi Zhen,[1] Xiang Ruan,[1] Yutao Liu,[1] Xianzeng Shi,[1,4] Dawei Man,[1,2,3] Xiaofang Kang,[1,2,3] and Guanghui Xia[1,2,3]

[1]*School of Civil Engineering, Anhui Jianzhu University, Hefei 230601, China*
[2]*BIM Engineering Center of Anhui Province, Hefei 230601, China*
[3]*Prefabricated Building Research Institute of Anhui Province, Hefei 230601, China*
[4]*College of Civil and Transportation Engineering, Hohai University, Nanjing 210098, China*

Correspondence should be addressed to Xianzeng Shi; shixianzeng@ahjzu.edu.cn

Received 9 December 2021; Accepted 26 January 2022; Published 27 February 2022

Academic Editor: Debiao Meng

This paper presents an overlapping decentralized guaranteed cost hybrid control method for adjacent buildings with uncertain parameters, by combining the guaranteed cost control algorithm with the overlapping decentralized control strategy. The passive dampers are used as link members between the two parallel buildings, and the active control devices are installed between two consecutive floors in two adjacent buildings. The passive coupling dampers modulate the relative responses between the two buildings, and the active control devices modulate the interstory responses of each building. Based on the inclusion principle, a large-scale structure is divided into a set of paired substructures with common parts first. Then, the controller of each pair of substructures is designed by using the guaranteed cost algorithm. After that, the controller of the original system is formed by using the contraction principle. Consequently, the proposed approach is used to prevent pounding damage and achieve the best results in earthquake response reduction of uncertain adjacent buildings when compared with the calculation results obtained by the centralized control strategy. Furthermore, the stability and reliability of the control system are promoted by adopting the overlapping decentralized control strategy.

1. Introduction

With rapid urbanization, an increasing number of adjacent buildings are appearing in cities. These buildings are usually separated from each other without connecting members, and their seismic performance of them depends on their characteristics. However, adjacent structures with insufficient spacing may collide with each other and cause more serious damage under earthquake excitation. For instance, the results of the investigation into the 1985 Mexico City earthquake showed that more than 40% of the 330 severely damaged buildings surveyed had collided with each other [1]. During the 1989 Loma Prieta City earthquake in the United States, over 200 of more than 500 buildings surveyed were destroyed by collision [2]. The Wenchuan earthquake in 2008 [3] and the Lushan earthquake in 2013 [4] caused adjacent buildings to be damaged by pounding. The inquiries on structural damage caused by the Christchurch earthquake in New Zealand in 2011 indicated that more than 6% of buildings had been severely destroyed by collision [5]. Previous earthquake damage investigations have shown that the collision damage to structures cannot be ignored. So, it has important research value to research how to improve the seismic performance of adjacent structures and avoid the occurrence of collision damage.

In recent years, the connected control method (CCM), which connects two independent structures by placing control equipment between adjacent buildings to resist external disturbances such as earthquakes, has attracted widespread attention from domestic and foreign scholars. The link members between adjacent buildings can adopt passive, active, or semiactive controllers [6]. CCM has been applied in mechanical, aerospace, and civil engineering fields, the study of which is of great significance. Now, CCM cannot only reduce the dynamic response of each structure but also effectively escape the occurrence of collision damage between adjacent structures [7]. Christenson et al. [8] used CCM to study the seismic response of adjacent buildings and discussed the influence of the ratio of building height on the control effect. Roh et al. [9] considered setting a combination of linear viscous dampers and linear springs between adjacent buildings to mitigate the seismic response of the structure and analyzed the influence of the ratio of adjacent building height, the ratio of fundamental periods, damping parameters of connected dampers, and external excitation of different frequencies on the story response. Patel and Jangid [10] optimized the number and damping coefficients of viscoelastic dampers which were adopted to link two adjacent multi-degree-of-freedom buildings. Cimellaro et al. [11] considered robust control algorithms to enhance the performance of adjacent structural models connected by passive dampers. Motra et al. [12] studied the problem of adjacent buildings linked by MR dampers with LQR control, considering a modified Bouc–Wen model that relates damping force to the input voltage state. Then, the response attenuation results were compared by employing LQR-RNN and LQR-CVL. Bigdeli et al. [13, 14] discussed the number and location of connecting dampers so that the performance of adjacent buildings can be promoted. Gao et al. [15] put forward a dynamic output feedback control method for mitigating structural seismic vibration and obtaining the location of the actuators and sensors, which were placed between adjacent buildings. Gudarzi and Zamanian [16] designed an output feedback controller based on the Kalman filter and optimal control theory for three adjacent buildings under earthquake action to provide a promising means of response attenuation. Yang and Lam [17] extensively studied the vibration of two eccentric adjacent buildings linked by viscoelastic dampers under bidirectional earthquakes. Uz and Hadi [18] introduced an optimization design method of nonlinear hysteretic dampers based on genetic algorithms [19] and demonstrated that the proper number of dampers was more helpful in improving the seismic performance of two adjacent buildings.

However, the centralized control strategy has flaws such as large computation, low reliability, and poor stability. Therefore, the decentralized control strategy with the advantages of fast data transmission, less feedback delay, and strong system reliability received extensive attention [20–23]. Especially, the focus of the research is on overlapping decentralized control strategies, based on the inclusion principle, which is a method to dispose of decentralized control of a large-scale system. This approach can effectively deal with the interconnection information between substructures and realize the decoupling of the system. Besides, it can also enhance the robustness and flexibility of controller design, when a large-scale system is decomposed into several low-order subsystems, and the subcontroller design is carried out through parallel computing. First of all, a large-scale system is divided into a series of paired subsystems based on the inclusion principle, in which shared information is considered. Then, a preset control algorithm is used to design the controller for the subsystem. Finally, the contraction principle is applied to contract the extended subsystem controller to form the controller of the original system [21–24]. Palacios-Quiñonero et al. [7, 25] studied an overlapping decentralized passive-active control method of adjacent buildings under an earthquake, which integrates the high performance of an active control system with the reliability of a passive control system and allows the decentralized design and operation of an active control subsystem.

Due to the influence of model errors, material deformation, external interference, and other factors, the structural model parameters are uncertain in practical engineering. Uncertainty-based design is becoming one of the research hotspots for engineering systems [26–28]. If the influence of uncertainty is not considered in the controller design, the control effect of the system will be difficult to guarantee. Therefore, the reliability of the system becomes especially important in various fields [29–35]. So, to improve the accuracy of modeling and ensure the stability of the control system, the constructed model is made to resemble the actual model by adding uncertainty influencing factors in the process of modeling. Chang and Peng [36] first proposed the guaranteed cost control method for uncertain systems in 1972 and successfully solved this problem. This method makes the performance functions of the system have a certain upper bound and can also ensure its robust stability. Bakule et al. [37, 38] adopted overlapping decentralized guaranteed cost control methods to analyze uncertain continuous time-delay systems and uncertain discrete time-delay systems. The references [39, 40] studied uncertain discrete state time-delay systems and uncertain discrete time-delay systems with both states and inputs while proposing a guaranteed cost control method based on bilinear matrix inequality. Gyurkovics et al. [41] discussed dynamic output feedback guaranteed cost control for uncertain discrete time-delay systems. Aiming at a class of uncertain linear systems, Ahmadi et al. [42] extended the original system to a weakly interconnected system that retains all the properties of the original system based on the inclusion principle. Then, the iterative linear matrix inequality (ILMI) algorithm was applied to design the static output feedback overlapping decentralized controller of the extended system, which eventually contracted into the overlapping decentralized guaranteed cost controller of the original system.

In this paper, an overlapping decentralized guaranteed cost hybrid control method, using the inclusion principle and the overlapping decentralized control scheme with the guaranteed cost control algorithm, has been established for uncertain parameter adjacent structure systems under earthquake. The guaranteed cost control algorithm is adopted in each subsystem to get their controller, which is contracted to the original state-space to obtain the overlapping decentralized controller, and the mitigation of responses between adjacent buildings is dependent on passive dampers linked by them. The method has been tested for two neighboring buildings with uncertain parameters, and the numerical analysis results are compared with those of the centralized guaranteed cost vibration control strategy to illustrate its effectiveness.

2. Hybrid Control of Overlapping Decentralized Guaranteed Cost for Systems with Uncertain Parameters

2.1. Systematic Description of Adjacent Buildings with Uncertain Parameters. Figure 1 shows the structural model of the adjacent buildings. Considering the uncertainties of the mass, stiffness, damping, and other factors of the structure, the motion equation of the controlled system is obtained:

$$(\mathbf{M}+\Delta\mathbf{M})\ddot{x}(t)+(\mathbf{C}+\Delta\mathbf{C})\dot{x}(t)+(\mathbf{K}+\Delta\mathbf{K})\mathbf{x}(t)=\mathbf{D}_s\ddot{x}_g(t)+\mathbf{B}_u\mathbf{u}(t), \tag{1}$$

where $\mathbf{M}$, $\mathbf{C}$, and $\mathbf{K}$ are the total mass, damping, and stiffness matrices of adjacent buildings, respectively; $\Delta\mathbf{M}$, $\Delta\mathbf{C}$, and $\Delta\mathbf{K}$ are the corresponding variation matrices, respectively; $\mathbf{D}_s$ and $\mathbf{B}_u$ are the position matrices of seismic excitation and control force, respectively; $\mathbf{x}(t)$ is the displacement vector of the structure; $\mathbf{u}(t)$ is the control force vector; and $\ddot{x}_g$ is the seismic acceleration. In Figure 1, m_i^j, c_i^j, and k_i^j denote the mass, damping coefficient, and interlayer shear stiffness, where i, l, r, and d represent the floor, the left building, the right building, and the passive dampers, respectively.where

$$\begin{aligned}
\mathbf{M}&=\begin{bmatrix}\mathbf{M}_L & \mathbf{0}\\ \mathbf{0} & \mathbf{M}_R\end{bmatrix},\\
\mathbf{M}_L&=\operatorname{diag}\left\{m_1^l, m_2^l, \ldots, m_{n_1-1}^l, m_{n_1}^l\right\},\\
\mathbf{M}_R&=\operatorname{diag}\left\{m_1^r, m_2^r, \ldots, m_{n_2-1}^r, m_{n_2}^r\right\},\\
\mathbf{K}&=\mathbf{K}_B+\mathbf{K}_D,
\end{aligned} \tag{2}$$

$$\begin{aligned}
\mathbf{K}_B&=\begin{bmatrix}\mathbf{K}_L & \mathbf{0}\\ \mathbf{0} & \mathbf{K}_R\end{bmatrix},\\
\mathbf{K}_D&=\begin{bmatrix}[\mathbf{k}_d]_{n_2\times n_2} & [\mathbf{0}]_{n_2\times(n_1-n_2)} & [-\mathbf{k}_d]_{n_2\times n_2}\\ [\mathbf{0}]_{(n_1-n_2)\times n_2} & [\mathbf{0}]_{(n_1-n_2)\times(n_1-n_2)} & [\mathbf{0}]_{(n_1-n_2)\times n_2}\\ [-\mathbf{k}_d]_{n_2\times n_2} & [\mathbf{0}]_{n_2\times(n_1-n_2)} & [\mathbf{k}_d]_{n_2\times n_2}\end{bmatrix},
\end{aligned} \tag{3}$$

$$\mathbf{K}_L=\begin{bmatrix}k_1^l+k_2^l & -k_2^l & & & & \\ -k_2^l & k_2^l+k_3^l & -k_3^l & & & \\ & -k_3^l & k_3^l+k_4^l & -k_4^l & & \\ & & \cdots & \cdots & \cdots & \\ & & & -k_{n_1-1}^l & k_{n_1-1}^l+k_{n_1}^l & -k_{n_1}^l\\ & & & & -k_{n_1}^l & k_{n_1}^l\end{bmatrix}, \tag{4}$$

$$\mathbf{K}_R=\begin{bmatrix}k_1^r+k_2^r & -k_2^r & & & & \\ -k_2^r & k_2^r+k_3^r & -k_3^r & & & \\ & -k_3^r & k_3^r+k_4^r & -k_4^r & & \\ & & \cdots & \cdots & \cdots & \\ & & & -k_{n_2-1}^r & k_{n_2-1}^r+k_{n_2}^r & -k_{n_2}^r\\ & & & & -k_{n_2}^r & k_{n_2}^r\end{bmatrix}, \tag{5}$$

$$\mathbf{k}_d=\operatorname{diag}\left\{k_1^d, k_2^d, \ldots, k_{n_2-1}^d, k_{n_2}^d\right\}, \tag{6}$$

$$\mathbf{C}=\mathbf{C}_B+\mathbf{C}_D. \tag{7}$$

The matrices $\mathbf{C}_B$ and $\mathbf{C}_D$ can be obtained by using equations (3)~(6) and replacing interlayer stiffness coefficient k_i^j with damping coefficient c_i^j. $\mathbf{M}_L$ and $\mathbf{K}_L$ are the mass and stiffness matrices of the building on the left, respectively; $\mathbf{M}_R$ and $\mathbf{K}_R$ are the mass and stiffness matrices of the building on the right, respectively; $\mathbf{K}_B$ and $\mathbf{C}_B$ are the stiffness and damping matrices of adjacent structures, respectively; and $\mathbf{K}_D$ and $\mathbf{C}_D$ are the stiffness and damping matrices of connected systems, respectively.

$$\begin{aligned}
\mathbf{x}(t)&=\left[x_1^l(t), x_2^l(t), \ldots, x_{n_1}^l(t), x_1^r(t), x_2^r(t), \ldots, x_{n_2}^r(t)\right]^T,\\
\mathbf{D}_s&=-(\mathbf{M}+\Delta\mathbf{M})[\mathbf{1}]_{(n_1+n_2)\times 1},\\
\mathbf{B}_u&=\begin{bmatrix}[\mathbf{B}_u^l]_{n_1\times n_1} & [\mathbf{0}]_{n_1\times n_2}\\ [\mathbf{0}]_{n_2\times n_1} & [\mathbf{B}_u^r]_{n_2\times n_2}\end{bmatrix},
\end{aligned} \tag{8}$$

where

$$\begin{aligned}
\mathbf{B}_u^l&=\begin{cases}\left(B_u^l\right)_{i,i}=1, & 1\le i\le n_1,\\ \left(B_u^l\right)_{i,i+1}=-1, & 1\le i< n_1,\\ \left(B_u^l\right)_{i,j}=0, & \text{else},\end{cases}\\
\mathbf{B}_u^r&=\begin{cases}\left(B_u^r\right)_{i,i}=1, & 1\le i\le n_2,\\ \left(B_u^r\right)_{i,i+1}=-1, & 1\le i< n_2,\\ \left(B_u^r\right)_{i,j}=0, & \text{else},\end{cases}\\
\mathbf{u}(t)&=\left[u_1^l(t), u_2^l(t), \ldots, u_{n_1}^l(t), u_1^r(t), u_2^r(t), \ldots, u_{n_2}^r(t)\right]^T,\\
\Delta\mathbf{M}&=\alpha\boldsymbol{\delta}_{\mathbf{M}}\mathbf{M},\\
\Delta\mathbf{C}&=\beta\boldsymbol{\delta}_{\mathbf{C}}\mathbf{C},\\
\Delta\mathbf{K}&=\gamma\boldsymbol{\delta}_{\mathbf{K}}\mathbf{K},
\end{aligned} \tag{9}$$

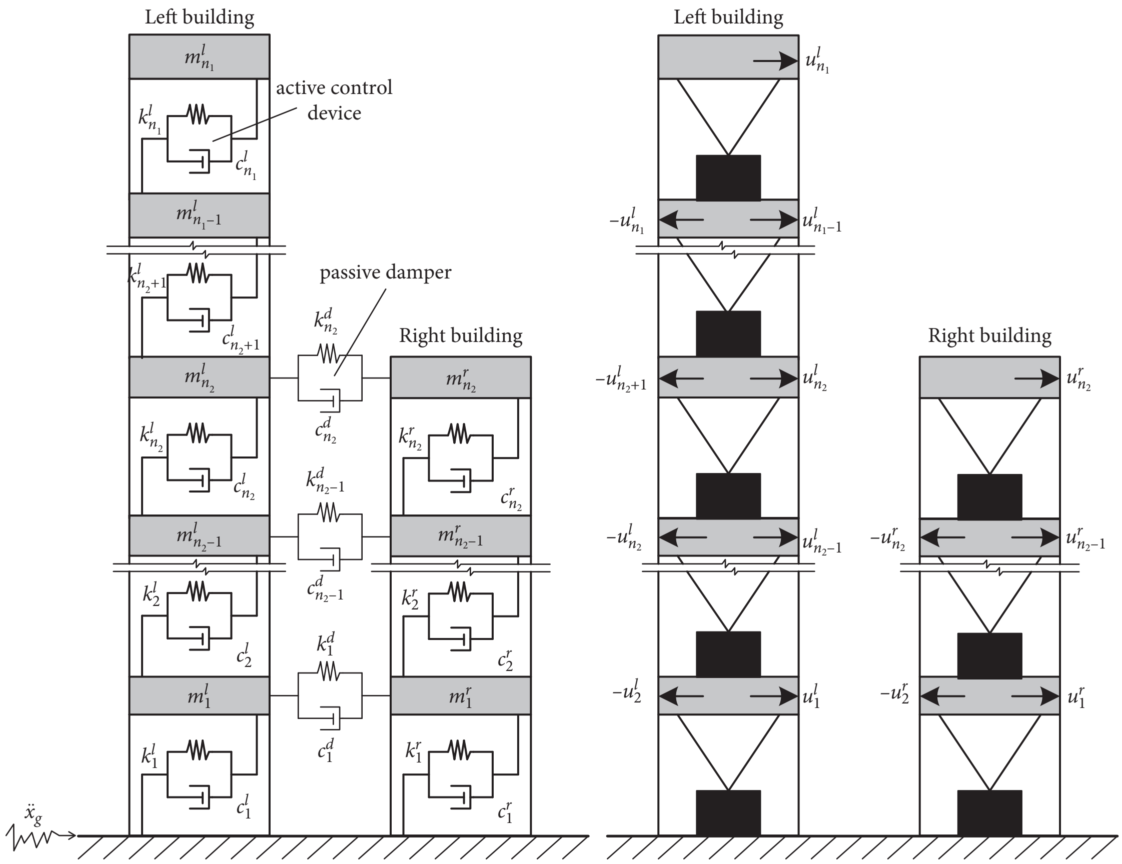

Figure 1: The model of adjacent buildings.

where α, β, and γ are the maximum rate of change of mass, damping, and stiffness, respectively. $\delta_{\mathbf{M}} = \begin{bmatrix} \delta_{\mathbf{M}_L} & \mathbf{0} \\ \mathbf{0} & \delta_{\mathbf{M}_R} \end{bmatrix}$, $\delta_{\mathbf{C}} = \begin{bmatrix} \delta_{\mathbf{C}_L} & \mathbf{0} \\ \mathbf{0} & \delta_{\mathbf{C}_R} \end{bmatrix}$, $\delta_{\mathbf{K}} = \begin{bmatrix} \delta_{\mathbf{K}_L} & \mathbf{0} \\ \mathbf{0} & \delta_{\mathbf{K}_R} \end{bmatrix}$, $\delta_{\mathbf{C}}$ and $\delta_{\mathbf{K}}$ are unknown real function matrices of appropriate dimensions. Since $\delta_{\mathbf{M}}$ is a diagonal matrix [43], so

$$\begin{aligned}(\mathbf{M} + \Delta\mathbf{M})^{-1} &= \mathbf{M}^{-1} + \Delta_1\mathbf{M} \\ \Delta_1\mathbf{M} &= -\left(\alpha\mathbf{M}^{-1}\right)\boldsymbol{\delta}_{\mathbf{M}}\left(\mathbf{I} + \alpha\boldsymbol{\delta}_{\mathbf{M}}\right)^{-1}.\end{aligned} \tag{10}$$

Equation (1) is transformed into a state-space model

$$\dot{Z}_p(t) = \left(\mathbf{A}_p + \Delta\mathbf{A}_p\right)\mathbf{Z}_p(t) + \left(\mathbf{B}_p + \Delta\mathbf{B}_p\right)\mathbf{u}(t) + \mathbf{E}_p\ddot{x}_g(t), \tag{11}$$

where

$$\begin{aligned}
\mathbf{A}_p &= \begin{bmatrix} \mathbf{0} & \mathbf{I} \\ -\mathbf{M}^{-1}\mathbf{K} & -\mathbf{M}^{-1}\mathbf{C} \end{bmatrix}, \\
\mathbf{B}_p &= \begin{bmatrix} \mathbf{0} \\ \mathbf{M}^{-1}\mathbf{B}_u \end{bmatrix}, \\
\mathbf{E}_p &= \begin{bmatrix} \mathbf{0} \\ -[\mathbf{1}] \end{bmatrix}, \\
\mathbf{Z}_p(t) &= \left[\, \mathbf{x}^l(t) \;\; \dot{x}^l(t) \;\; \mathbf{x}^r(t) \;\; \dot{x}^r(t) \,\right]^T, \\
\Delta\mathbf{A}_p &= \begin{bmatrix} \mathbf{0} & \mathbf{0} \\ -\Delta_{\mathbf{MK}} & -\Delta_{\mathbf{MC}} \end{bmatrix}, \\
\Delta\mathbf{B}_p &= \begin{bmatrix} \mathbf{0} \\ \Delta_1\mathbf{MB}_u \end{bmatrix}, \\
\Delta_{\mathbf{MK}} &= \Delta_1\mathbf{M}(\mathbf{K} + \Delta\mathbf{K}) + \mathbf{M}^{-1}\Delta\mathbf{K}, \\
\Delta_{\mathbf{MC}} &= \Delta_1\mathbf{M}(\mathbf{C} + \Delta\mathbf{C}) + \mathbf{M}^{-1}\Delta\mathbf{C}, \\
\left(\Delta\mathbf{A}_p \;\; \Delta\mathbf{B}_p\right) &= \mathbf{D}_p\mathbf{F}_p\left(\mathbf{E}_{p1} \;\; \mathbf{E}_{p2}\right).
\end{aligned} \tag{12}$$

We define a new state vector $\mathbf{Z}(t) = \overline{T}\mathbf{Z}_p(t)$, where

$$\overline{T}=\begin{bmatrix}\overline{T}^{l} & \mathbf{0}\\ \mathbf{0} & \overline{T}^{r}\end{bmatrix},$$

$$\overline{T}^{l}=\begin{cases}\overline{T}^{l}_{1,1}=1, & \overline{T}^{l}_{2,n_1+1}=1\\ \overline{T}^{l}_{2i-1,i-1}=-1, & \overline{T}^{l}_{2i-1,i}=1, \quad 1<i\leq n_1\\ \overline{T}^{l}_{2i,\mathrm{n}_1+i-1}=-1, & \overline{T}^{l}_{2i,\mathrm{n}_1+i}=1, \quad 1<i\leq n_1\\ \overline{T}^{l}_{i,j}=0, & else\end{cases},$$

$$\overline{T}^{r}=\begin{cases}\overline{T}^{r}_{1,1}=1, & \overline{T}^{r}_{2,n_2+1}=1\\ \overline{T}^{r}_{2i-1,i-1}=-1, & \overline{T}^{r}_{2i-1,i}=1, \quad 1<i\leq n_2\\ \overline{T}^{r}_{2i,\mathrm{n}_2+i-1}=-1, & \overline{T}^{r}_{2i,\mathrm{n}_2+i}=1, \quad 1<i\leq n_2\\ \overline{T}^{r}_{i,j}=0, & \text{else}\end{cases},\tag{13}$$

$$\mathbf{Z}(t)=\begin{bmatrix}x_1^l(t),\dot{x}_1^l(t),\,(x_2^l(t)-x_1^l(t)),\left(\dot{x}_2^l(t)-\dot{x}_1^l(t)\right),\ldots,\left(x_{n_1}^l(t)-x_{n_1-1}^l(t)\right),\left(\dot{x}_{n_1}^l(t)-\dot{x}_{n_1-1}^l(t)\right),\\ x_1^r(t),\dot{x}_1^r(t),\,(x_2^r(t)-x_1^r(t)),\,(\dot{x}_2^r(t)-\dot{x}_1^r(t)),\ldots,\left(x_{n_2}^r(t)-x_{n_2-1}^r(t)\right),\left(\dot{x}_{n_2}^r(t)-\dot{x}_{n_2-1}^r(t)\right)\end{bmatrix}^T.$$

The new state-space model can be expressed as

$$\dot{Z}(t)=(\mathbf{A}+\Delta\mathbf{A})\mathbf{Z}(t)+(\mathbf{B}+\Delta\mathbf{B})\mathbf{u}(t)+\mathbf{E}\ddot{x}_g(t),\tag{14}$$

where

$$\begin{aligned}\mathbf{A}&=\overline{T}\mathbf{A}_p\overline{T}^{-1},\\ \mathbf{B}&=\overline{T}\mathbf{B}_p,\\ \mathbf{E}&=\overline{T}\mathbf{E}_p,\\ \Delta\mathbf{A}&=\overline{T}\Delta\mathbf{A}_p\overline{T}^{-1},\\ \Delta\mathbf{B}&=\overline{T}\Delta\mathbf{B}_p.\end{aligned}\tag{15}$$

2.2. System Extension. Consider the following state-space model of a linearly continuous time-invariant system

$$\begin{aligned}\mathbf{S}&:\ \dot{Z}(t)=(\mathbf{A}+\Delta\mathbf{A})\mathbf{Z}(t)+(\mathbf{B}+\Delta\mathbf{B})\mathbf{u}(t),\\ &\quad\ \mathbf{y}(t)=\mathbf{C_y}\mathbf{Z}(t),\\ \widetilde{\mathbf{S}}&:\ \dot{\widetilde{Z}}(t)=(\widetilde{A}+\Delta\widetilde{A})\widetilde{Z}(t)+(\widetilde{B}+\Delta\widetilde{B})\widetilde{u}(t),\\ &\quad\ \widetilde{y}(t)=\widetilde{C}_y\widetilde{Z}(t),\end{aligned}\tag{16}$$

where $\mathbf{Z}(t)\in\mathbf{R}^n$, $\mathbf{u}(t)\in\mathbf{R}^m$, and $\mathbf{y}(t)\in\mathbf{R}^l$ are the state, input vector, and output vector of the system $\mathbf{S}$, respectively. $\widetilde{Z}(t)\in\mathbf{R}^{\widetilde{n}}$, $\widetilde{u}(t)\in\mathbf{R}^{\widetilde{m}}$, and $\widetilde{y}(t)\in\mathbf{R}^{\widetilde{l}}$ are the state, input vector, and output vector of the system $\widetilde{\mathbf{S}}$, respectively. $\mathbf{A}$, $\mathbf{B}$, $\mathbf{C}_y$ and $\widetilde{A}$, $\widetilde{B}$, and $\widetilde{C}_y$ are $n\times n$, $n\times m$, $l\times n$, $\widetilde{n}\times\widetilde{n}$, $\widetilde{n}\times\widetilde{m}$, and $\widetilde{l}\times\widetilde{n}$ dimensional matrices, respectively. $n\leq\widetilde{n}, m\leq\widetilde{m}, l\leq\widetilde{l}$. Based on the inclusion principle [21], for a linear uncertain system $\mathbf{S}$, a set of extended matrices $\mathbf{V}$, $\mathbf{R}$, and $\mathbf{T}$, and a set of shrinkage matrices $\mathbf{U}$, $\mathbf{Q}$, and $\mathbf{S}$, the corresponding extended system $\widetilde{\mathbf{S}}$ can be expressed as follows:

$$\begin{aligned}\widetilde{A}&=\mathbf{VAU}+\mathbf{M},\\ \widetilde{B}&=\mathbf{VBQ}+\mathbf{N},\\ \widetilde{C}_y&=\mathbf{TC}_y\mathbf{U}+\mathbf{L},\\ \Delta\widetilde{A}&=\mathbf{V}\Delta\mathbf{AU},\\ \Delta\widetilde{B}&=\mathbf{V}\Delta\mathbf{BQ},\end{aligned}\tag{17}$$

where $\mathbf{M}, \mathbf{N}$, and $\mathbf{L}$ are the compensation matrices [21, 44].

The system $\mathbf{S}$ is decomposed into L fully decoupled paired subsystems by extending decoupling [21].

$$\begin{aligned}\widetilde{\mathbf{S}}_D^{(i)}&:\ \dot{\widetilde{Z}}_i(t)=\left(\widetilde{A}_{ii}+\Delta\widetilde{A}_{ii}\right)\widetilde{Z}_i(t)+\left(\widetilde{B}_{ii}+\Delta\widetilde{B}_{ii}\right)\widetilde{u}_i(t),\\ &\quad\ \widetilde{y}_i(t)=\left(\widetilde{C}_y\right)_{ii}\widetilde{Z}_i(t),\quad i=1,2,\ldots,L,\end{aligned}\tag{18}$$

where $\widetilde{A}_{ii}$ and $\widetilde{B}_{ii}$ are known constant matrices describing the system model. $\Delta\widetilde{A}_{ii}$ and $\Delta\widetilde{B}_{ii}$ are unknown matrices that represent the parameter uncertainty in the system model. It is assumed that the parameter uncertainty under consideration is norm-bounded and has the following form:

$$\left[\Delta\widetilde{A}_{ii}\ \ \Delta\widetilde{B}_{ii}\right]=\widetilde{D}_i\widetilde{F}_i(t)\left[\widetilde{E}_{i1}\ \ \widetilde{E}_{i2}\right],\tag{19}$$

where $\widetilde{D}_i$, $\widetilde{E}_{i1}$, and $\widetilde{E}_{i2}$ are matrices of constants, which reflect uncertain structural information, $\widetilde{F}_i(t)$ is an unknown matrix, and $\widetilde{F}_i^T(t)\widetilde{F}_i(t)\leq\mathbf{I}$.

2.3. Design of Guaranteed Cost Controller. It is assumed that system $\widetilde{\mathbf{S}}_D^{(i)}$ meets the quadratic performance metric

$$\widetilde{J}_i\left(\widetilde{Z}_i,\widetilde{u}_i\right)=\int_0^\infty\left[\widetilde{Z}_i^T(t)\widetilde{Q}_i^*\widetilde{Z}_i(t)+\widetilde{u}_i^T(t)\widetilde{R}_i^*\widetilde{u}_i(t)\right]\mathrm{d}t,\tag{20}$$

where $\widetilde{Q}_i^*$ and $\widetilde{R}_i^*$ are given symmetric positive definite weighted matrices.

Theorem 1 (see [45]). *For the parameter uncertainty subsystem $\widetilde{\mathbf{S}}_D^{(i)}$ and performance index (20), if the following optimization problem*

$$\min_{\widetilde{\varepsilon}_i,\widetilde{Y}_i,\widetilde{X}_i,\widetilde{W}_i} \operatorname{Trace}(\widetilde{W}_i),$$

$$\text{s.t.}\quad (i)\begin{bmatrix} \widetilde{A}_{ii}\widetilde{X}_i + \widetilde{B}_{ii}\widetilde{Y}_i + \left(\widetilde{A}_{ii}\widetilde{X}_i + \widetilde{B}_{ii}\widetilde{Y}_i\right)^{\mathrm{T}} + \widetilde{\varepsilon}_i\widetilde{D}_i\widetilde{D}_i^{\mathrm{T}} & \left(\widetilde{E}_{i1}\widetilde{X}_i + \widetilde{E}_{i2}\widetilde{Y}_i\right)^{\mathrm{T}} & \widetilde{X}_i & \widetilde{Y}_i^{\mathrm{T}} \\ \widetilde{E}_{i1}\widetilde{X}_i + \widetilde{E}_{i2}\widetilde{Y}_i & -\widetilde{\varepsilon}_i\mathbf{I} & 0 & 0 \\ \widetilde{X}_i & 0 & -\left(\widetilde{Q}_i^*\right)^{-1} & 0 \\ \widetilde{Y}_i & 0 & 0 & -\left(\widetilde{R}_i^*\right)^{-1} \end{bmatrix} < 0, \tag{21}$$

$$(\mathrm{ii})\begin{bmatrix} \widetilde{W}_i & \mathbf{I} \\ \mathbf{I} & \widetilde{X}_i \end{bmatrix} > 0,$$

has a solution $(\widetilde{\varepsilon}_i, \widetilde{Y}_i, \widetilde{X}_i, \widetilde{W}_i)$, then $\widetilde{u}_i^*(t) = \widetilde{Y}_i\widetilde{X}_i^{-1}\widetilde{Z}_i(t)$ is the optimal state feedback guaranteed cost control law of the system, where $\widetilde{\varepsilon}_i$ denotes a scalar greater than 0. $\widetilde{X}_i$ and $\widetilde{W}_i$ denote symmetric positive definite matrix, $\widetilde{Y}_i$ denotes a matrix of appropriate dimensions. The gain matrix of subsystem decentralized controller is $\widetilde{G}_i = \widetilde{Y}_i\widetilde{X}_i^{-1}$.

2.4. Contraction of the System. The overlapping decentralized hybrid control method is a design method that combines the passive connected damping units between adjacent buildings with the overlapping decentralized active control systems of each building. For the extended decoupling system $\widetilde{\mathbf{S}}_D^{(i)}, i = (1, 2, \ldots, L)$, the feedback gain matrices $\widetilde{G}_i$ of all subsystems are calculated by using the control algorithm, represented as a block diagonal matrix

$$\widetilde{G} = \operatorname{diag}\left[\widetilde{G}_1, \widetilde{G}_2, \ldots, \widetilde{G}_L\right]. \tag{22}$$

The extension controller $\widetilde{G}$ can be contracted to an overlapping controller based on the contraction principle [21, 44], i.e.,

$$\mathbf{G} = \mathbf{Q}\widetilde{G}\mathbf{V}. \tag{23}$$

3. Example Simulation and Analysis

Taking 4-story and 5-story adjacent buildings (as shown in Figure 2) as an example, the corresponding parameters of the adjacent structures can be seen in reference [46].

The damping matrix is determined according to the Rayleigh damping, and the damping ratio is set to 2%. The damping coefficient of the viscous damper connecting the two structures is $c_d = 6.87 \times 10^6 N \cdot s/m$, and the stiffness coefficient is 0. The linked damper is located between the 4th floor of the two buildings.

Northridge seismic wave is used as external excitation, and its peak value is $3.0\,m/s^2$, duration is 30 s, and sampling step is 0.02 s.

Only structural stiffness variation is taken into account in this calculation example, and the maximum possible variation of stiffness is ±15% [47]. In (9), let $\alpha = \beta = 0$, so $\Delta\mathbf{M} = \Delta\mathbf{C} = \mathbf{0}$ and $\Delta\mathbf{K} = \gamma\,\mathbf{K}$, where $\mathbf{K}$ represents the nominal stiffness matrices and $\gamma = 0.15$ reflects the variation of stiffness matrix, then

$$\begin{aligned} \Delta\mathbf{A}_p^l &= \mathbf{D}_p^l\mathbf{F}_p^l\mathbf{E}_{p1}^l, \\ \Delta\mathbf{B}_p^l &= \mathbf{0}, \\ \mathbf{D}_p^l &= \begin{bmatrix} \mathbf{0} \\ -\mathbf{M}_L^{-1}\mathbf{K}_L \end{bmatrix}_{2n_1\times n_1}, \\ \mathbf{F}_p^l &= \delta[\mathbf{I}]_{2n_1\times 2n_1}, \\ \mathbf{E}_{pl}^l &= [\,\mathbf{I}\ \ \mathbf{0}\,]_{n_1\times 2n_1}, \end{aligned} \tag{24}$$

δ is an uncertain real scalar, $|\delta| < 1$.

In the same way, we can get $\Delta\mathbf{A}_p^r, \Delta\mathbf{B}_p^r, \Delta\mathbf{D}_p^r$, $\Delta\mathbf{F}_p^r$, $\Delta\mathbf{E}_{p1}^r$, and $\Delta\mathbf{E}_{p2}^r$.

3.1. Centralized Control. Centralized control adopts the state feedback guaranteed cost control method in Theorem 1 to design the controller for the whole multistructure system. The weighting matrices of the building on the left are $\mathbf{Q}_1^l = 1 \times 10^2\mathbf{I}_8$ and $\mathbf{R}_1^l = 10^{-10}\mathbf{I}_4$. The weighting matrices of the building on the right are $\mathbf{Q}_1^l = 1 \times 10^2\mathbf{I}_{10}$ and $\mathbf{R}_1^l = 10^{-10}\mathbf{I}_5$.

$\mathbf{G}^l$ and $\mathbf{G}^r$ can be obtained by solving inequality (21); then, the gain matrix of the whole multistructure structure system can be expressed as $\mathbf{G} = \operatorname{diag}\left\{\mathbf{G}^l, \mathbf{G}^r\right\}$.

3.2. Overlapping Decentralized Control. The inclusion principle is applied to perform overlapping decomposition of the adjacent buildings, and then controller design is carried out, as shown in Figure 3. Extended decoupling of the two buildings separately: system $\widetilde{S}_1^l = [1, 2, 3]$, system $\widetilde{S}_2^l = [3, 4]$, system $\widetilde{S}_1^r = [1, 2, 3]$, and system $\widetilde{S}_2^r = [3, 4, 5]$. The overlapping layers are all set at the third layer of the structure. The state-space model of the subsystem can be expressed in the form of equation (18).

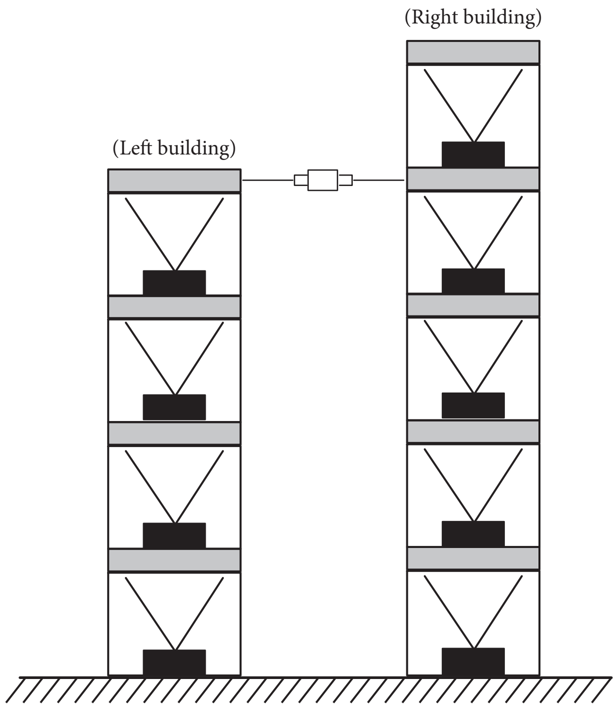

FIGURE 2: The model of 4-story and 5-story adjacent buildings.

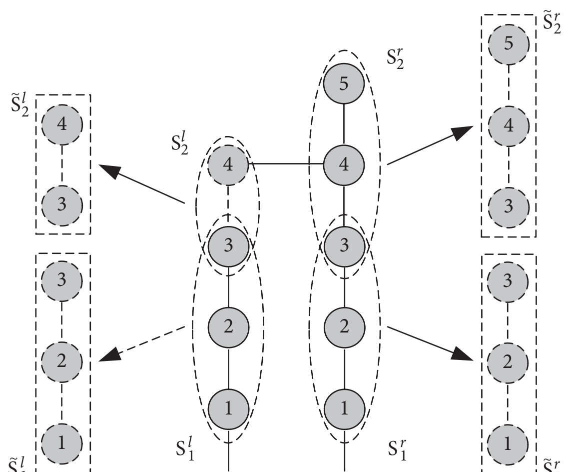

FIGURE 3: The design of overlapping decentralized controller.

Through the trial, the weighted matrices of the system $\tilde{S}_1^l$ and $\tilde{S}_2^l$ are $(\tilde{Q}_1^l)^* = 1.0 \times 10^2 \mathbf{I}_6$, $(\tilde{R}_1^l)^* = 10^{-10}\mathbf{I}_3$, $(\tilde{Q}_2^l)^* = 1.0 \times 10^2 \mathbf{I}_4$, and $(\tilde{R}_2^l)^* = 10^{-10}\mathbf{I}_2$; the weighted matrices of the system $\tilde{S}_1^r$ and $\tilde{S}_2^r$ are $(\tilde{Q}_1^r)^* = 8.0 \times 10^2 \mathbf{I}_6$, $(\tilde{R}_1^r)^* = 10^{-10}\mathbf{I}_3$, $(\tilde{Q}_2^r)^* = 1.0 \times 10^2 \mathbf{I}_6$, and $(\tilde{R}_2^r)^* = 10^{-10}\mathbf{I}_3$. Solving the linear matrix inequality (LMI) according to Theorem 1, we can get $\tilde{\varepsilon}_i^l$, $\tilde{Y}_i^l$, $\tilde{X}_i^l$, $\tilde{W}_i^l$ and $\tilde{\varepsilon}_i^r$, $\tilde{Y}_i^r$, $\tilde{X}_i^r$, $\tilde{W}_i^r$. The gain matrices of the building subsystem on the left are $\tilde{G}_1^l = \tilde{Y}_1^l(\tilde{X}_1^l)^{-1}$ and $\tilde{G}_2^l = \tilde{Y}_2^l(\tilde{X}_2^l)^{-1}$. The gain matrices of the building subsystem on the right are $\tilde{G}_1^r = \tilde{Y}_1^r(\tilde{X}_1^r)^{-1}$ and $\tilde{G}_2^r = \tilde{Y}_2^r(\tilde{X}_2^r)^{-1}$.

The gain matrices of the system $\tilde{S}^l$ and $\tilde{S}^r$ are expressed as block diagonal matrix, so $\tilde{G}^l = \mathrm{diag}\{\tilde{G}_1^l, \tilde{G}_2^l\}$ and $\tilde{G}^r = \mathrm{diag}\{\tilde{G}_1^r, \tilde{G}_2^r\}$. The gain matrices of the original system $\mathbf{S}^l$ and $\mathbf{S}^r$ are obtained according to the contraction principle, so $\mathbf{G}^l = \mathbf{Q}^l\tilde{G}^l\mathbf{V}^l$ and $\mathbf{G}^r = \mathbf{Q}^r\tilde{G}^r\mathbf{V}^r$; then, the gain matrix of the entire multistructure system can be expressed as $\mathbf{G} = \mathrm{diag}\{\mathbf{G}^l, \mathbf{G}^r\}$.

3.3. Analysis of Calculation Results. Figures 4–6 show the peak interlayer displacement of adjacent buildings with uncertain parameters.

It can be seen from the figure that, for the building on the left, (1) when $\Delta K = 0$, the average control effect of centralized guaranteed cost hybrid control method (CHC) is 66.94%, and the average control effect of overlapping decentralized guaranteed cost hybrid control approach (ODHC) is 74.68%; (2) when $\Delta K = +0.15\,\mathrm{K}$, the average control effect of centralized guaranteed cost control method is 66.58%, and the average control effect of overlapping decentralized guaranteed cost hybrid control approach is 72.33%; and (3) when $\Delta K = -0.15\,\mathrm{K}$, the average control effect of centralized guaranteed cost control method is 65.88%, and the average

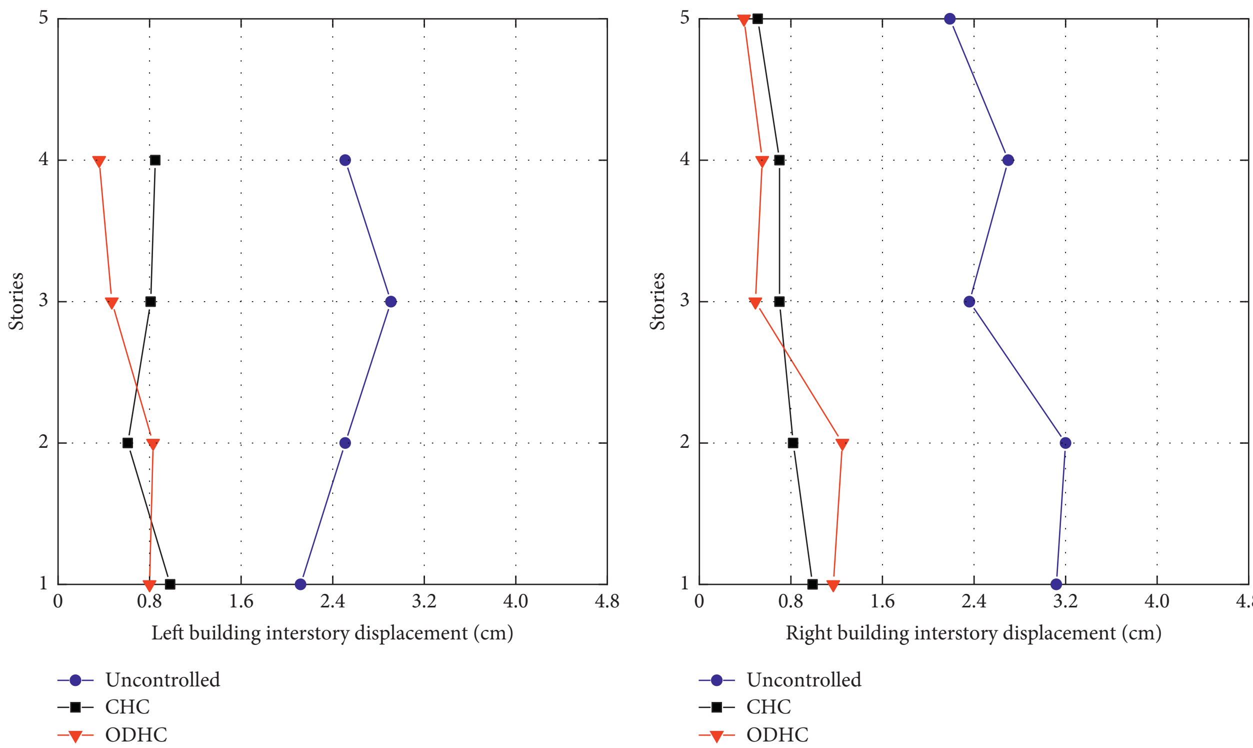

(a) (b)

Figure 4: The peak interstory displacement ($\Delta K = 0$): (a) the left building; (b) the right building.

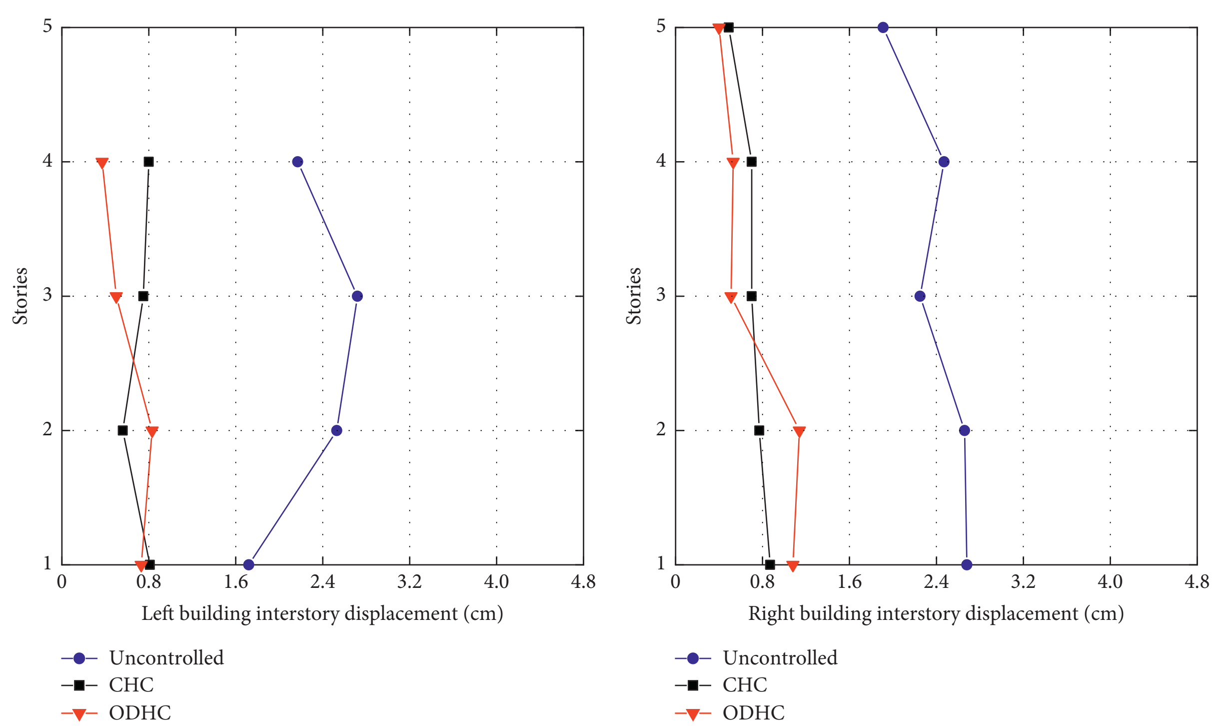

(a) (b)

Figure 5: The peak interstory displacement ($\Delta K = +0.15\,K$): (a) the left building; (b) the right building.

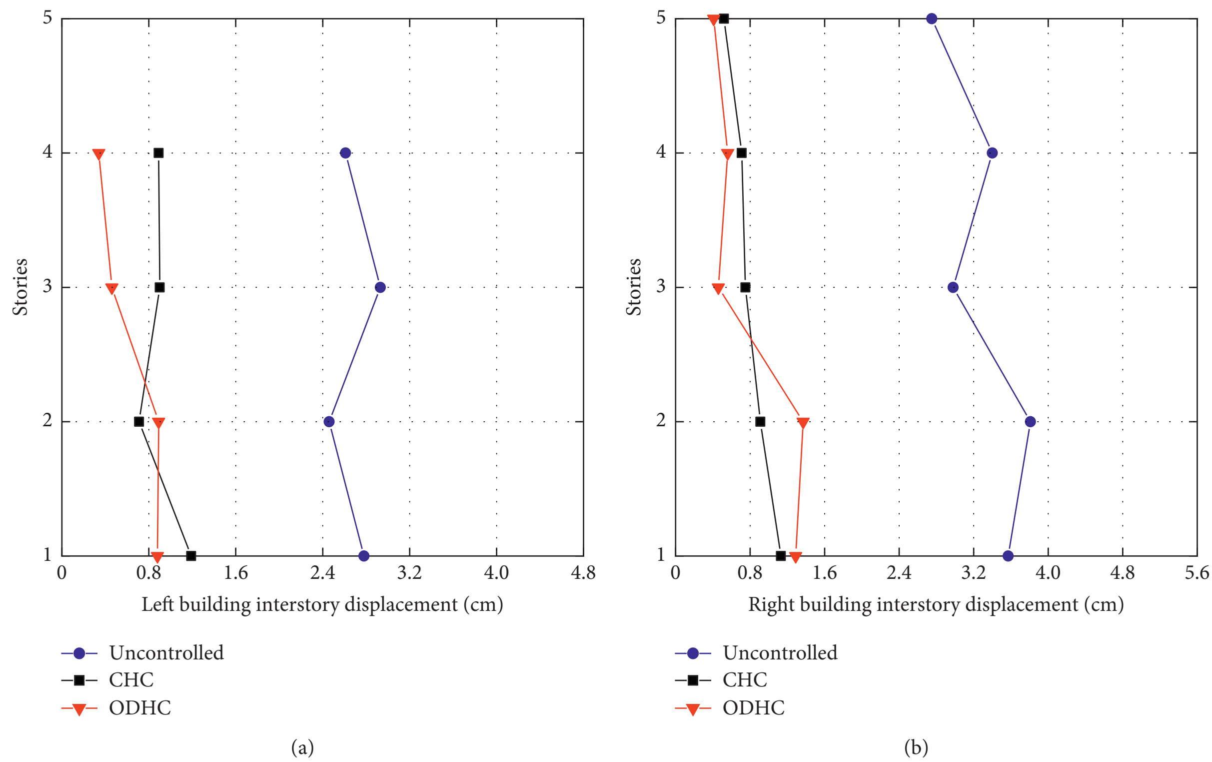

Figure 6: The peak interstory displacement ($\Delta K = -0.15\,K$): (a) the left building; (b) the right building.

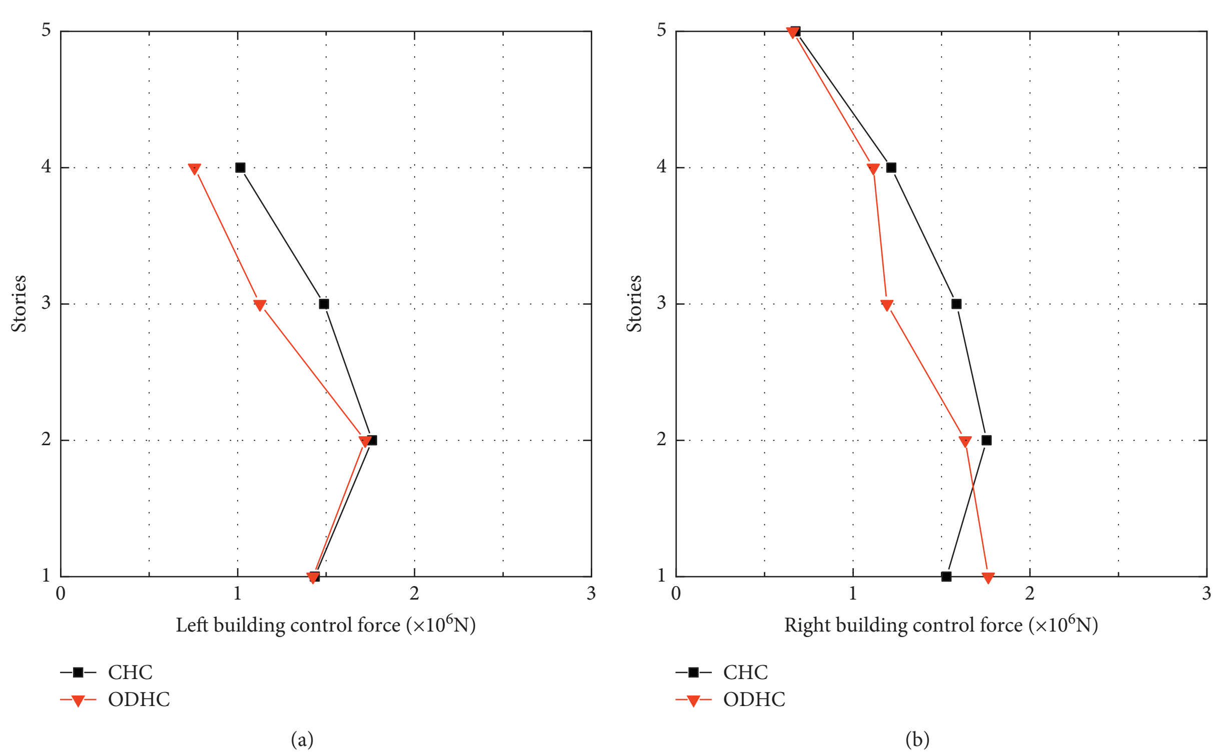

Figure 7: Maximum control forces ($\Delta K = 0$): (a) the left building; (b) the right building.

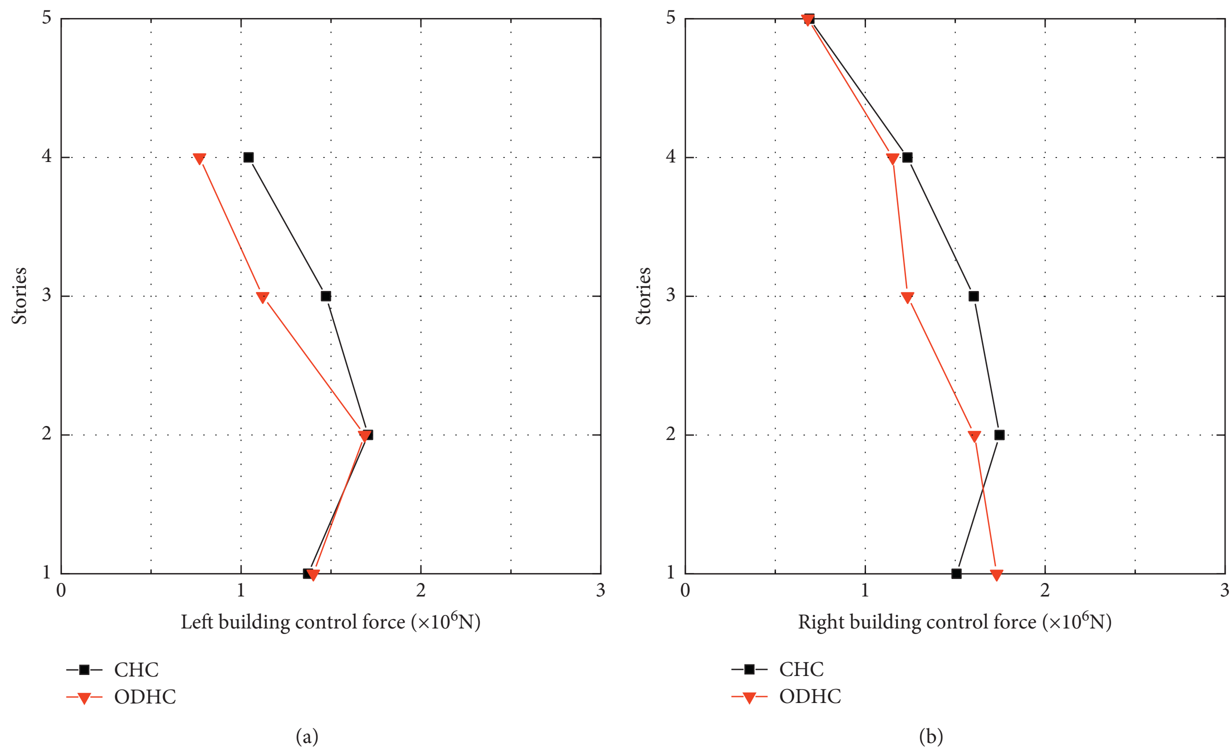

FIGURE 8: Maximum control forces ($\Delta K = +0.15\,K$): (a) the left building; (b) the right building.

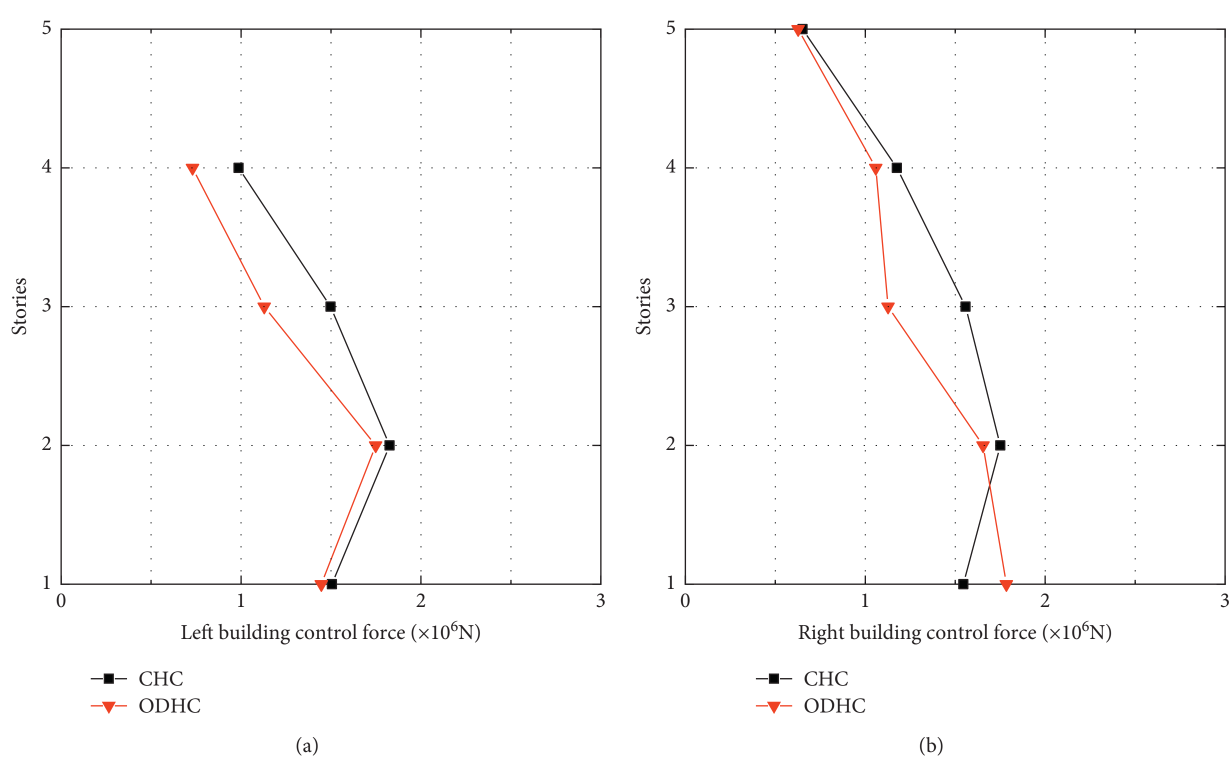

FIGURE 9: Maximum control forces ($\Delta K = -0.15\,K$): (a) the left building; (b) the right building.

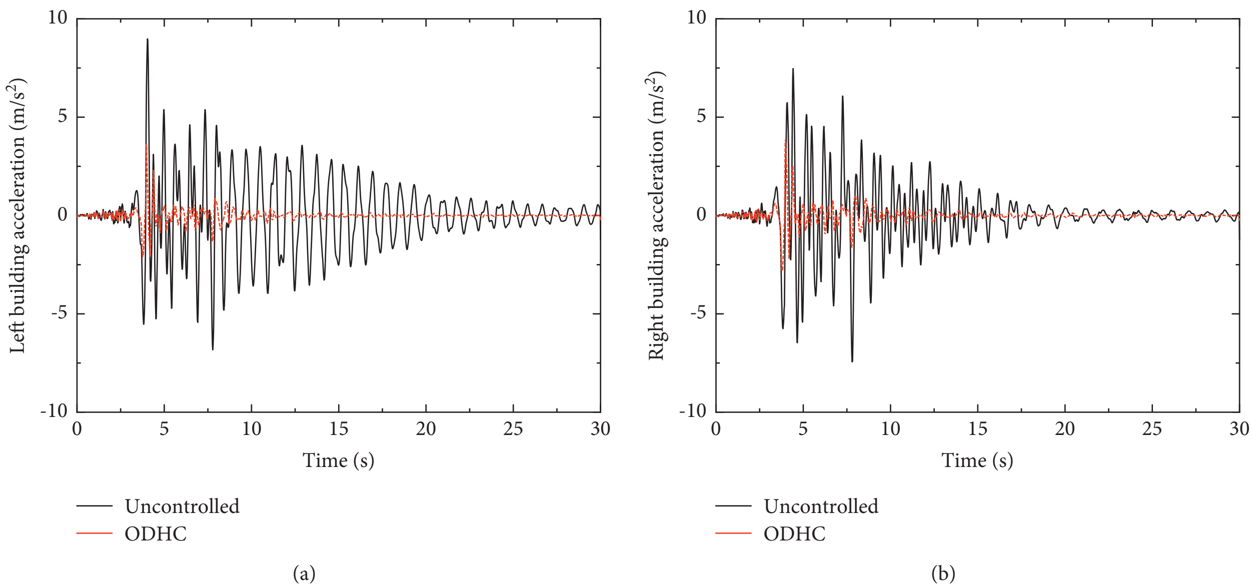

Figure 10: Acceleration time-history curves of the top floor ($\Delta K = 0$): (a) the left building; (b) the right building.

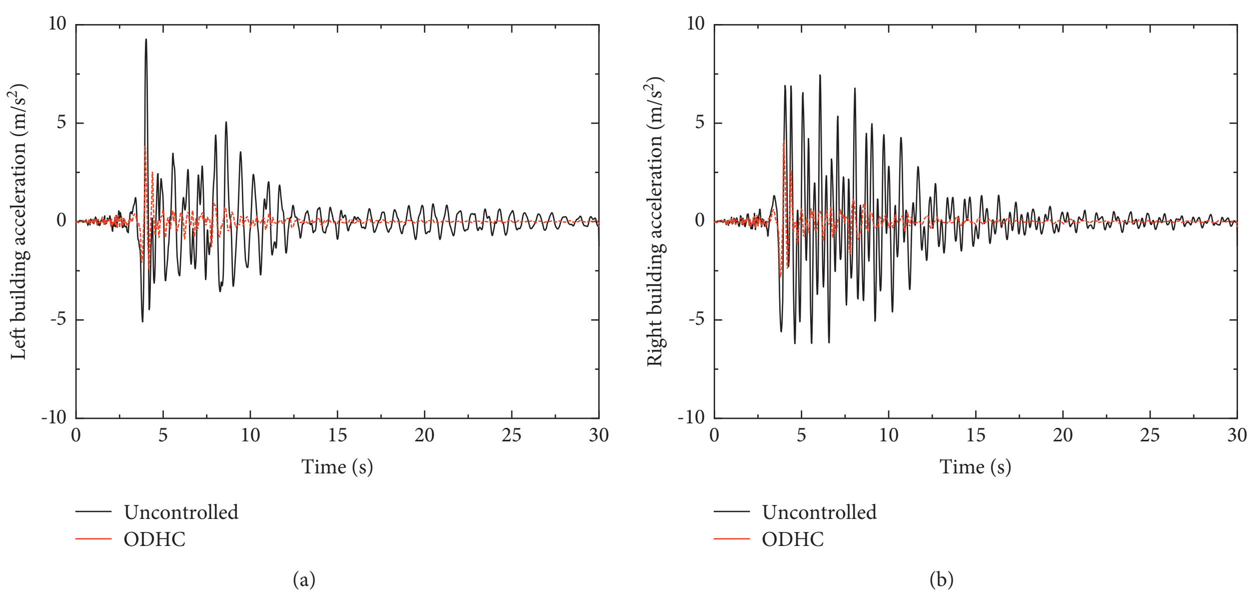

Figure 11: Acceleration time-history curves of the top floor ($\Delta K = +0.15\,\mathrm{K}$): (a) the left building; (b) the right building.

control effect of overlapping decentralized guaranteed cost hybrid control approach is 75.86%.

For the building on the right, (1)when $\Delta K = 0$, the average control effect of centralized guaranteed cost control method is 72.75%, and the average control effect of overlapping decentralized guaranteed cost hybrid control approach is 72.90%; (2)when $\Delta K = +0.15\,\mathrm{K}$, the average control effect of centralized guaranteed cost control method is 70.70%, and the average control effect of overlapping decentralized guaranteed cost hybrid control approach is 70.36%; and (3)when $\Delta K = -0.15\,\mathrm{K}$, the average control effect of centralized guaranteed cost control method is 75.90%, and the average control effect of overlapping decentralized guaranteed cost hybrid control approach is 76.22%.

Figures 7–12 show the maximum control force and acceleration response of uncertain adjacent building systems under seismic excitation. From Figures 7–9, it can be seen that the maximum control force of the ODHC method is not much different from that of the CHC method.

It can be seen from Figures 10–12 that the ODHC method can still effectively control the acceleration response of the structure in the case of variation of structural parameters, which illustrates the effectiveness of the ODHC method proposed in this paper.

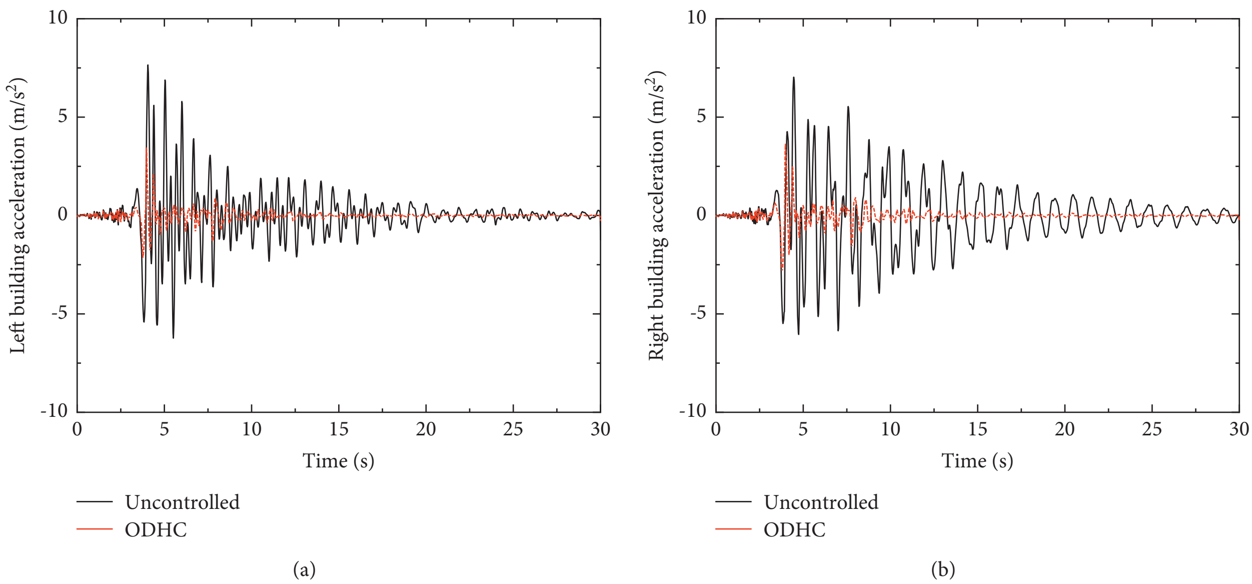

FIGURE 12: Acceleration time-history curves of the top floor ($\Delta K = -0.15\,K$): (a) the left building; (b) the right building.

4. Conclusions

In this paper, a new scheme to solve the problem of structural vibration control for adjacent buildings with uncertain parameters has been proposed. The pilot studies in exploring overlapping decentralized guaranteed cost hybrid control design, which integrates the high performance of active control system with the reliability of the passive control system, while allowing the decentralized design and operation of the active control subsystem, that combines the overlapping decentralized control strategy and the guaranteed cost control algorithm via LMI are carried out. The main findings are summarized as follows:

(1) The centralized control strategy can effectively analyze the structural vibration control problem, while the overlapping decentralized control strategy provides a new idea. The LMI is used as a tool that makes the design of the guaranteed cost controller easier to solve. Numerical simulation results using uncertain parameters for 4-story and 5-story adjacent buildings illustrate the feasibility of the proposed control approach, which can still effectively reduce the seismic response of a multistructure system when the structural parameters are uncertain.

(2) A comparison of performance between the overlapping decentralized guaranteed cost controllers and the centralized guaranteed cost controllers indicates that both controllers deliver the expected effect. Meanwhile, the proposed control method in this paper can improve the sampling rate and data transmission speed to ensure the reliability of the adjacent system.

(3) The overlapping decentralized control design, which overcomes the disadvantages of traditional centralized control strategies such as large computation, low reliability, and poor stability, offers promising solutions to complex structural systems.

Data Availability

The data used to support the study are available from the corresponding authors upon request.

Conflicts of Interest

The authors declare that there are no conflicts of interest regarding the publication of this paper.

Acknowledgments

This study was financially supported by the Natural Science Research Project of Higher Education Institutions in Anhui Province (KJ2019A0748, KJ2019A0747, and KJ2020A0490), the Doctoral Startup Foundation of Anhui Jianzhu University (2018QD28, 2017QD05, 2020QDZ07, and 2020QDZ38), the Anhui Provincial Natural Science Foundation (2008085QE245 and 2108085QA41), the Project of Science and Technology Plan of Department of Housing and Urban-Rural Development of Anhui Province (2019YF-029, 2020-YF20, and 2021-YF22), the National College Student Innovation and Entrepreneurship Training Program Project (202110878060), and the School-Enterprise Cooperative Development Project of Anhui Jianzhu University (HYB20190137).

References

[1] K. Kasai, V. Jeng, P. C. Patel, J. A. MunShi, and B. F. Maison, "Seismic pounding effects-survey and analysis," in *Proceedings of the 10th World Conference on Earthquake Engineering*, pp. 3893–3898, Madrid, Spain, July 1992.

[2] K. Kasai and B. F. Maison, "Building pounding damage during the 1989 Loma Prieta earthquake," *Engineering Structures*, vol. 19, no. 3, pp. 195–207, 1997.

[3] Z. Wang, "A preliminary report on the great wenchuan earthquake," *Engineering and Engineering Vibration*, vol. 7, no. 2, pp. 225–234, 2008.

[4] Y. Q. Yang, J. W. Dai, M. S. Gong, and L. L. Xie, "Investigation and analysis on adjacent buildings pounding damage in Lushan earthquake," *Journal of Harbin Institute of Technology*, vol. 47, no. 12, pp. 102–105, 2015, (in Chinese).

[5] G. L. Cole, R. P. Dhakal, F. M. Turner, and F. M. Turner, "Building pounding damage observed in the 2011 Christchurch earthquake," *Earthquake Engineering & Structural Dynamics*, vol. 41, no. 5, pp. 893–913, 2012.

[6] F. Palacios-Quiñonero, J. M. Rossel, J. Rubió-Massegú, and H. R. Karimi, "Structural vibration control for a class of connected multistructure mechanical systems," *Mathematical Problems in Engineering*, vol. 2012, Article ID 942910, 23 pages, 2012.

[7] F. Palacios-Quinonero, J. M. Rossel, J. Rodellar, and H. R. Karimi, "Active-passive control strategy for adjacent buildings," in *Proceedings of the American Control Conference (ACC)*, pp. 3110–3115, San Francisco, CA, USA, July 2011.

[8] R. E. Christenson, B. F. Spencer, and E. A. Johnson, "Semi-active connected control method for adjacent multidegree-of-freedom buildings," *Journal of Engineering Mechanics*, vol. 133, no. 3, pp. 290–298, 2007.

[9] H. Roh, G. P. Cimellaro, and D. Lopez-Garcia, "Seismic response of adjacent steel structures connected by passive device," *Advances in Structural Engineering*, vol. 14, no. 3, pp. 499–517, 2011.

[10] C. C. Patel and R. S. Jangid, "Seismic response of dynamically similar adjacent structures connected with viscous dampers," *The IES Journal Part A: Civil & Structural Engineering*, vol. 3, no. 1, pp. 1–13, 2010.

[11] G. P. Cimellaro and D. Lopez-Garcia, "Algorithm for design of controlled motion of adjacent structures," *Structural Control and Health Monitoring*, vol. 18, no. 2, pp. 140–148, 2011.

[12] G. B. Motra, W. Mallik, and N. K. Chandiramani, "Semi-active vibration control of connected buildings using magnetorheological dampers," *Journal of Intelligent Material Systems and Structures*, vol. 22, no. 16, pp. 1811–1827, 2011.

[13] K. Bigdeli, W. Hare, and S. Tesfamariam, "Configuration optimization of dampers for adjacent buildings under seismic excitations," *Engineering Optimization*, vol. 44, no. 12, pp. 1491–1509, 2012.

[14] K. Bigdeli, W. Hare, J. Nutini, and S. Tesfamariam, "Optimizing damper connectors for adjacent buildings," *Optimization and Engineering*, vol. 17, no. 1, pp. 47–75, 2016.

[15] H. J. Gao, X. B. Yang, W. Zhan, and H. R. Karimi, "Actuators and sensors allocation for adjacent buildings vibration control," in *Proceedings of the 38th Annual Conference on IEEE Industrial Electronics Society*, pp. 4821–4826, Montreal, QC, USA, October 2012.

[16] M. Gudarzi and H. Zamanian, "Application of active vibration control for earthquake protection of multi-structural buildings," *International Journal of Scientific Research in Knowledge*, vol. 1, no. 11, pp. 502–513, 2013.

[17] Z. Yang and E. S. S. Lam, "Dynamic responses of two buildings connected by viscoelastic dampers under bidirectional earthquake excitations," *Earthquake Engineering and Engineering Vibration*, vol. 13, no. 1, pp. 137–150, 2014.

[18] M. E. Uz and M. N. S. Hadi, "Optimal design of semi active control for adjacent buildings connected by MR damper based on integrated fuzzy logic and multi-objective genetic algorithm," *Engineering Structures*, vol. 69, pp. 135–148, 2014.

[19] R. Yuan, H. Q. Li, and Q. U. Wang, "An enhanced genetic algorithm–based multi-objective design optimization strategy," *Advances in Mechanical Engineering*, vol. 10, no. 7, pp. 1–6, 2018.

[20] X. F. Kang, J. G. Wang, and Q. Wang, "Study on the building structural overlapping decentralized control based on energy-to-peak control algorithm," *Chinese Journal of Applied Mechanics*, vol. 32, no. 6, pp. 9 55–961, 2015, (in Chinese).

[21] F. Palacios-Quiñonero, J. M. Rossell, and H. R. Karimi, "Semi-decentralized strategies in structural vibration control," *Modeling Identification and Control*, vol. 32, no. 2, pp. 57–77, 2011.

[22] Q. Wang, J. L. Zhuang, J. Zhang, and J. G. Wang, "Overlapping decentralized control of tall buildings under earthquakes," *Chinese Journal of Computational Mechanics*, vol. 32, no. 1, pp. 48–52, 2015, (in Chinese).

[23] R. Yuan and H. Q. Li, "A multidisciplinary coupling relationship coordination algorithm using the hierarchical control methods of complex systems and its application in multidisciplinary design optimization," *Advances in Mechanical Engineering*, vol. 9, no. 1, pp. 1–11, 2017.

[24] H. R. Karimi, F. Palacios-Quiñonero, J. M. Rossell, and J. Rubió-Massegú, "Sequential design of multioverlapping controllers for structural vibration control of tall buildings under seismic excitation," *Proceedings of the Institution of Mechanical Engineers - Part I: Journal of Systems & Control Engineering*, vol. 227, no. 2, pp. 176–183, 2013.

[25] F. Palacios-Quiñonero, J. Rodellar Benedé, J. M. Rossell Garriga, and J. Rubió-Massegú, "Control strategies for large-scale structural systems: high-raise buildings and multi-building systems," in *Proceedings of the Workshop on Control, Dynamics, Monitoring and Applications*, pp. 40–56, Barcelona, Spain, February 2011.

[26] H. Li, R. Yuan, and J. Fu, "A reliability modeling for multi-component systems considering random shocks and multi-state degradation," *IEEE Access*, vol. 7, pp. 168805–168814, 2019.

[27] P. P. Zhi, Y. Xu, and B. Z. Chen, "Time-dependent reliability analysis of the motor hanger for EMU based on stochastic process," *International Journal of Structural Integrity*, vol. 11, no. 3, pp. 453–469, 2020.

[28] R. Yuan, H. Q. Li, Z. C. Gong, M. Z. Tang, and W. Li, "An enhanced Monte Carlo simulation–based design and optimization method and its application in the speed reducer design," *Advances in Mechanical Engineering*, vol. 9, no. 9, pp. 1–7, 2017.

[29] R. Yuan, H. Q. Li, and Q. U. Wang, "Simulation-based design and optimization and fatigue characteristics for high-speed backplane connector," *Advances in Mechanical Engineering*, vol. 11, no. 6, pp. 1–10, 2019.

[30] L. Abdullah, S. S. Karam Singh, A. H. Azman, S. Abdullah, A. K. A. Mohd Ihsan, and Y. S. Kong, "Fatigue life-based reliability assessment of a heavy vehicle leaf spring," *International Journal of Structural Integrity*, vol. 10, no. 5, pp. 726–736, 2019.

[31] R. Manouchehry Nya, S. Abdullah, and S. Singh Karam Singh, "Reliability-based fatigue life of vehicle spring under random loading," *International Journal of Structural Integrity*, vol. 10, no. 5, pp. 737–748, 2019.

[32] A. A. Abd Rahim, S. Abdullah, S. Singh Karam Singh, and M. Z. Nuawi, "Reliability assessment on automobile suspension system using wavelet analysis," *International journal of structural integrity*, vol. 10, no. 5, pp. 602–611, 2019.

[33] R. Yuan, M. Tang, H. Wang, and H. Li, "A reliability analysis method of accelerated performance degradation based on Bayesian strategy," *IEEE Access*, vol. 7, pp. 169047–169054, 2019.

[34] M. Nahal and R. Khelif, "A finite element model for estimating time-dependent reliability of a corroded pipeline elbow," *International Journal of Structural Integrity*, vol. 12, no. 2, pp. 306–321, 2021.

[35] Y.-J. Yang, G. Wang, Q. Zhong, H. Zhang, J. He, and H. Chen, "Reliability analysis of gas pipeline with corrosion defect based on finite element method," *International Journal of Structural Integrity*, vol. 12, no. 6, pp. 854–863, 2021.

[36] S. Chang and T. Peng, "Adaptive guaranteed cost control of systems with uncertain parameters," *IEEE Transactions on Automatic Control*, vol. 17, no. 4, pp. 474–483, 1972.

[37] L. Bakule, J. Rodellar, and J. M. Rossell, "Robust overlapping guaranteed cost control of uncertain state-delay discrete-time systems," *IEEE Transactions on Automatic Control*, vol. 51, no. 12, pp. 1943–1950, 2006.

[38] L. Bakule and J. M. Rossell, "Overlapping controllers for uncertain delay continuous-time systems," *Kybernetika*, vol. 44, no. 1, pp. 17–34, 2008.

[39] X. Nian, Z. Sun, H. Wang, H. Zhang, and X. Wang, "Bilinear matrix inequality approaches to robust guaranteed cost control for uncertain discrete-time delay system," *Optimal Control Applications and Methods*, vol. 34, no. 4, pp. 433–441, 2013.

[40] X. Zhou, T. Dong, X. Tang, C. Yang, and W. Gui, "A BMI approach to guaranteed cost control of discrete-time uncertain system with both state and input delays," *Optimal Control Applications and Methods*, vol. 36, no. 6, pp. 844–852, 2015.

[41] E. Gyurkovics and T. Takacs, "Guaranteed cost for uncertain discrete-time delay systems," *Control Applications of Optimization*, vol. 15, no. 1, pp. 106–111, 2012.

[42] A. Ahmadi, M. Aldeen, and M. Abdolmaleki, "Robust overlapping output feedback control design in uncertain systems with unknown uncertainty bounds," in *Proceedings of the 5th Australian Control Conference (AUCC)*, pp. 69–74, Gold Coast, Australia, November 2015.

[43] S. J. Kim and J. W. Choi, "Parametric uncertainty in controlling the vibration of a building," in *Proceedings of the 39th SICE Annual Conference*, pp. 107–122, lizuka, Japan, July 2000.

[44] X.-B. Chen, W.-B. Xu, T.-Y. Huang, X.-Y. Ouyang, and S. S. Stankovic, "Pair-wise decomposition and coordinated control of complex systems," *Information Sciences*, vol. 185, no. 1, pp. 78–99, 2012.

[45] L. Yu, *Robust Control, Linear Matrix Inequality Approach*, Tsinghua University Press, Beijing, China, (in Chinese), 2002.

[46] F. Palacios-Quiñonero, J. Rubió-Massegú, J. M. Rossell, and H. R. Karimi, "Vibration control for adjacent structures using local state information," *Mechatronics*, vol. 24, no. 4, pp. 336–344, 2014.

[47] V. B. Patil and R. S. Jangid, "Optimum multiple tuned mass dampers for the wind excited benchmark building/optimalūs masės slopintuvai vėjo veikiamuose aukštybiniuose pastatuose," *Journal of Civil Engineering and Management*, vol. 17, no. 4, pp. 540–557, 2011.